Joint Active Passive Sensing using a Radio Frequency System-on-a-Chip based sensor

M. Ritchie, N. Peters, C. Horne
Dept. of Electronic and Electrical Engineering
University College London (UCL)
London, UK
m.ritchie@ucl.ac.uk

***Abstract*—In this paper we present a dual active and passive radar experimental setup that uses the UCL ARESTOR platform. This is a multi-role RF sensor based on a Xilinx Radio Frequency System on a Chip (RFSoC) device. The system is capable of operating as an active radar, passive radar and wideband electronic surveillance receiver. Experimental results are shown that leverage 2.4 GHz passive radar experiments along with a 5.8 GHz active radar mode that are operating simultaneously observing a target of interest. Details of a bespoke designed RF front-end to access higher frequency bands are included within the paper as well as information on processing pipelines developed within the Field Programmable Gate Array (FPGA). Comparison of the target signature and how both modes could be best utilised are analysed and discussed. The target of interest within this paper is a person walking while being sensing by both modes simultaneously.**

***Index Terms*—Active Radar, Passive Radar, FPGA, RFSoC, Fusion**

I. Introduction

Traditional Radio Frequency (RF) sensing typically uses very specific sensors designed for singular roles. With the current trend of pressure on RF spectrum availability, as well as modern battle-space congested & contested RF scenarios, there is a need for a step change in how RF sensing is undertaken. Our proposed system, ARESTOR, is a multi-role device capable of completing a number of tasks which would traditionally be undertaken by separate devices. The hardware is based around the Xilinx RF System on a Chip (RFSoC) while the software is a bespoke developed platform. This device is a Field Programmable Gate Array (FPGA) device which also incorporates high-speed Analog to Digital Converters (ADCs), Digital to Analog converters (DACs), two multi-core processors and multiple digital input and output (I/O) options. The result is a system that can operate as an active radar, passive radar, Electronic Surveillance (ES) and communication device. This single device can now satisfy multiple different requirements bringing many benefits including reduced costs, modularity, scalability as well as many others.

Previous UCL work using the ARESTOR system was shown in two papers, the first [1] first described the system, and the second [2] showed FMCW active radar mode only results linked to Unmanned Aerial Vehicle (UAV) experiments that covered 2 simultaneous bands (S & C). Within this paper for the first time simultaneous active and passive measurements at different frequencies bands are shown, along with the first description of a new bespoke RF front end design that works in conjunction with the ARESTOR platform to extend its transmit and receive frequencies. Data of a moving target is shown within the results where the joint sensing mode results have been overlaid to compare outputs.

This paper, in Section II, describes the concept behind the multi-role RF sensor platform and the developments required to create such a system, then details background literature in the area. Section III goes on to describe the experimental configuration and shows the capture results from the dual mode setup and finally Section IV highlights the conclusions from the presented results.

II. Background

The Xilinx RFSoC device was first released in 2018 [3] and represents a step change in commercially available devices that include integrated FPGA, ADCs and DACs which can be exploited as the digital back-end to a wide variety of applications. The area of advanced digital and software defined hardware has seen a great rise in capability in recent years. Prior released Software Defined Radio (SDR) solutions include the USRP [4], LimeSDR [5] and BladeRF [6] which are all very capable devices and have been applied to both active and passive radar sensing problems. In comparison the RFSoC hardware represents orders of magnitude greater sampling rates in both ADC and DAC as well as a powerful Digital Signal Processing (DSP) capabilities. This combination is a real enabler for many different devices and has therefore seen its rise in interest from the RF sensing research and development community. For example, the RFSoC was proposed as a suitable digital back-end solution for an active radar within [7]. Its advanced capabilities come at the cost of added complexity and challenging requirements on the broad range of technical skills required to develop on the RFSoC compared to some other solutions which provide template or simpler interfaces in order to control and develop on them.

Passive radar has been a fundamentally important area of radar research for many decades. The diversity of modern illuminators of opportunity (IoOs) presents a wide range

of passive radar applications. Short range and through wall passive sensing has been enabled by WiFi standards in both 2.4 GHz and 5 GHz bands. Whereas long range aircraft detection has been successfully achieved via waveforms such as DVB-T, FM and DAB [8]. Each IoO has different advantages and disadvantages and must be considered within the context of the target, geometry and receiver capabilities when designing a system. Within this work the passive IoO was 2.4 GHz, but the methodologies are applicable to other potential IoOs.

A challenge, in a real world scenario, where the RF sensor is in a 100% mission critical role, is that passive radar may rely on a non co-operative illuminator. This may not be acceptable and an active radar solution will instead be deployed. By developing a system that can operate in both modes a trade off decision can be made between WHEN to sense actively and WHEN to sense passively. This trade-off lends itself well to the area of cognitive radar by way of Haykin's perception action cycle [9]. The ARESTOR platform described within this publication, as a flexible dual active-passive sensor, would be able to start experimentally addressing these questions moving the concept of cognitive sensing to a higher Technology Readiness Level (TRL).

Very few joint active and passive sensing systems exist in the open literature. A range of multistatic radar systems that use a co-operative radar waveforms have been developed, for example the NetRAD & NeXtRAD radars [10], but systems that combine an active radar and a passive radar that leverages communications IoO are very rare. Some analysis has been performed on simulated concepts based on the principle that a distributed active and passive network of sensors are deployed [11]. This work shows how important geometry and node selection is when fusing the results from such a network. In addition recent research, [12], has a modelled result of a RF sensor network which combines both active and passive nodes. This work also introduced interference within the scenario to try and evaluate how this affects overall fusion of both range and Doppler estimation.

III. Experimental System and Results

The UCL ARESTOR hardware, Fig. 1 is based around the ZCU111 evaluation board from Xilinx [3]. This board features a first generation RFSoC device that has eight ADCs operating at 4 GS/s and eight DACs operating at 6.5 GS/s. Further generations of the RFSoC hardware are now available (up to 3rd gen), but the focus with ARESTOR so far has been to develop the RF sensing modalities on the first generation which could potentially be ported to higher generations if the requirements of a specific scenario required it.

For simultaneous active and passive radar measurements, it is highly desirable for the active radar to operate at a different frequency to the passive one. This prevents leakage from the relatively high-power active radar transmit from masking the comparatively low-power target returns in the passive radar. The maximum operating frequency of the first generation RFSoC device is 4 GHz, which is somewhat restrictive for joint active passive experiments, especially when aiming to

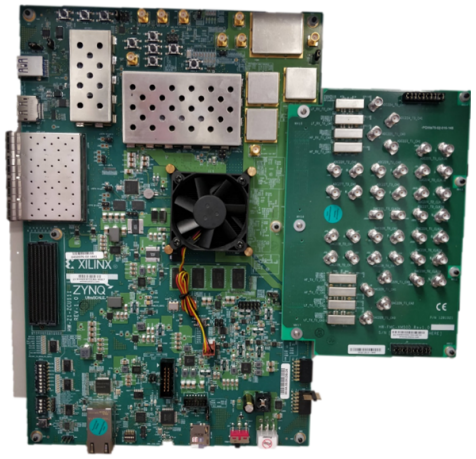

Fig. 1. Xilinx ZCU111 RFSoC which the ARESTOR system is based around.

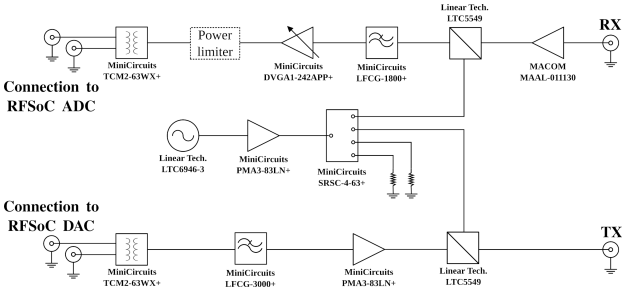

Fig. 2. Block diagram showing the design of the prototype RF front-end.

use two separate ISM bands (S and C band in this case) to allow experiments to be performed without a spectrum license. To overcome this limitation, we designed and constructed a prototype analog front-end for the RFSoC to expand its operational frequency range. The prototype provides wideband (2 - 13 GHz, 1.8 GHz bandwidth) up- and down-mixing for a single transmit and receive channel respectively and is connected to the differential-pair inputs/outputs of the RFSoC via short coaxial cables. Figure 2 shows a block diagram of the front-end design including the components selected to achieve wideband operation. The front-end includes an RF power limiting circuit to prevent excessive signal levels from damaging the ADCs on the RFSoC. Details of this circuit have been omitted from Fig. 2 for clarity. The implemented prototype is shown in Fig. 3 along with its supporting hardware (clocking, power supply unit (PSU) and control).

To reduce the cost of the front-end it was manufactured on low-cost FR4 dielectric. Although cheap, this dielectric is not suitable for high-frequency signals as it has a very high loss tangent and poorly constrained dielectric constant, resulting in high losses. These effects have been partially mitigated by keeping the RF traces on the printed circuit boards (PCBs) as short as possible. However, as shown in Fig. 4, the performance of our prototype degrades rapidly above 6 GHz. The data plotted in Fig. 4 were collected by sequentially transmitting intermediate frequency (IF) tones of

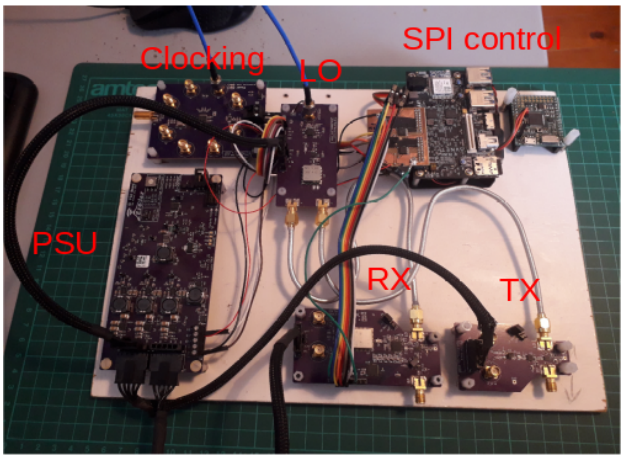

Fig. 3. Photo of the prototype RF front-end. The prototype is split across several separate PCBs, their functions are captioned in the image. Control of the front-end is via a Serial Peripheral Interface (SPI) bus, this is currently provided by an Avnet Ultra96 board, but in future versions will be driven by the RFSoC itself. The connections to the RFSoC are not shown in this image.

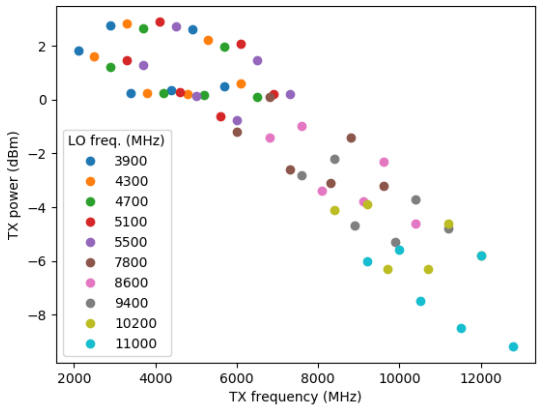

Fig. 4. Plot of RF front-end transmit power against frequency for different LO settings.

0.5, 1.0 and 1.8 GHz from the RFSoC, mixing with a specific local oscillator (LO) frequency on the front-end and measuring the power level of the two mixing sidebands using a spectrum analyser. It is interesting to note that for a given transmit frequency, there is a ∼3 dB variation in power that can be achieved by varying the LO and IF frequency. This is likely due to the variation in output power of the LO and RFSoC with frequency.

Future work will look to implement a second iteration of the front-end design on more suitable PCB dielectric to improve its high-frequency performance. For this study however, the prototype was sufficient to implement an active-radar using the 5.8 GHz ISM band. We selected an LO frequency of 4.275 GHz and an IF linear chirp between 1.45-1.6 GHz. A Mini-Circuits ZVBP-5800-S+ cavity filter was used to select the lower mixing sideband, resulting in a transmitted 150 MHz chirp centred at 5.8 GHz. A Mini-Circuits ZVA-183-S+ power amplifier was used to increase the transmit power to ∼22 dBm.

FMCW radar architectures typically use a component of the transmitted signal to mix directly with the received signal immediately after the antenna resulting in a beat frequency. This beat frequency has a much reduced sampling requirement compared to the full RF bandwidth of the original chirp and hence enables FMCW systems to have reduce cost and complexity. The ARESTOR system could also be configured in this way but for flexibility of design and to allow the system to rapidly change between either active or passive sensing modes it was configured to digitize the full bandwidth of the chirp and mix digitally with the transmitted signal but using a second channel that was simultaneously also sampled via a loop back connection. This is wasteful in terms of increasing the overall sampled data by orders of magnitude but the trade off is worth the flexibility. The systems is also capable of operating as pulsed Doppler radar and this mixing prior to digitisation would not be desired in that mode. If the system was only going to be a FMCW radar then analog mixing of the received signal to produce the beat frequency element prior to sampling would be used.

A key challenge when developing using a multiple Giga-samples per second (GSPS) system is the transfer of samples across the hardware at each interface. There is significant demand for multi-GHz radar solutions in order to benefit from the fine resolution that this enables but this puts very significant demands on the hardware capability to allow throughput of this data. The RFSoC evaluation board has a number of I/O options to transfer this data off the device. For these measurements, recorded data was stored onboard the RFSoC in DDR memory and transferred to an external hard-disc after each experiment. To reduce the size of the data files of the active radar mode the data stored has been de-ramped (mixed with the transmitted waveform) and decimated. Details of the transfer of data into DDR memory are given in [1].

The experimental setup used to acquire the results shown here is seen in Fig. 5. A WiFi router was deployed as the illuminator of opportunity at a distance of 4 m from the ARESTOR system. It uses a omni directional antenna which is provided with the router itself and ensures that signals are received directly at the reference antenna as well as scattering off the moving target in the scene back to the surveillance channel antenna. The MGEN tool [13] was used to stimulate the router over a established LAN to transmit continuously using 40 MHz bandwidth. This is important for passive radar as the level of activity of the communications channel affects the performance of the passive radar. In the scenario when broadcast communications signals are used (e.g. DVB-T) the signals are constantly active, while a WiFi LAN network requires stimulation in order to achieve a suitable waveform for passive radar. The position of the WiFi router was favourable for passive radar as it enabled us to isolate the separate reference and surveillance channels. Passive radar performance is very geometry dependent and if the target was in line with the illuminator source then poor performance would occur, hence the planned deployment that was used.

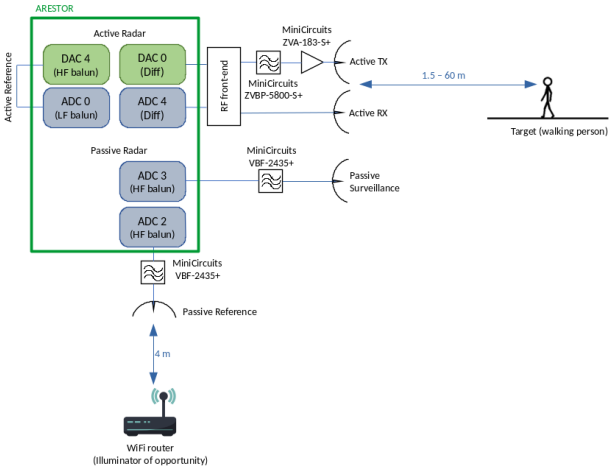

Fig. 5. Diagram of the experimental setup used for joint active-passive sensing using ARESTOR. Experiment geometry is shown, along with ADC and DAC allocations and the external components used.

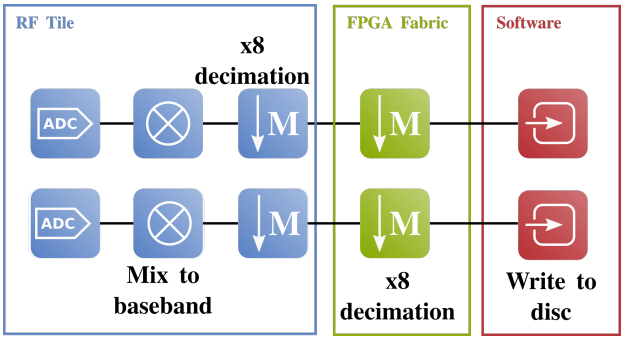

Fig. 6. Block diagram of the digital processing chain for the passive radar showing the partitioning of processing steps between different elements of the RFSoC.

Future work will look to investigate performance as a function of geometry and when it is best to use each of the modes. The target in this scenario was a person walking away from the radar approximately along the boresight of the active radar and approximately at right angles to the WiFi source. The range of the target varied from 1.5m to 60m. Little background clutter was present due to the trials site in an open field environment.

The passive radar receiver consisted of two receive channels, a reference channel directed straight at the router and a surveillance channel observing the target in the scene (perpendicular to the reference channel). Since the maximum sampling frequency of the RFSoC ADCs is 4 GS/s and the WiFi router was operating in the 2.4 GHz band we used super-Nyquist sampling, necessitating the use of external band-pass filters to reject any signals not in the second Nyquist zone. Data acquired on the passive channels was digitally down-mixed to baseband and then decimated by a factor of 8 twice (once using the built-in decimators on the RFSoC's RF tile and once using soft-IP decimators implemented in the FPGA fabric). This resulted in a complex signal sampled at 60 MHz, a significant data-reduction compared to saving the raw ADC samples. The real-time digital processing chain implemented on the RFSoC for the passive radar receiver is shown in Fig. 6. Processing of the passive data was done offline using Python scripts based on the PyApril software [14]. The primary processing steps for the passive radar outputs are (i) direct interference suppression (DSI) which attempts to remove interference by applying a Sample Matrix Inversion, Minimum Redundancy Estimation filter on the time domain surveillance data stream using the reference data stream, (ii) cross-correlation of the DSI filtered surveillance data stream with the reference data stream to identify delayed instances of the reference signal within the surveillance data, and (iii) a modified implementation of the PyApril constant false alarm rate (CFAR) processing, which better handles the near zero range target detection as compared with the original version, to detect target instances. The correlation step uses a segmented correlation approach inspired by Smith et. al. [15] which breaks the data stream into segments allowing only a fraction of the data to be correlated. The original purpose of this processing described in [15] was to extend the range coverage of passive radar without increasing processing load, in our work we use it to provide a reduction in processing load, at the cost of reduced processing gain.

The ARESTOR active radar was operated simultaneously along with the passive receiver channels. It used two DAC channels to transmit identical Linear Frequency Modulated (LFM) chirps with a period of 0.1 ms. A pulse repetition frequency of 5 kHz was used. One channel was looped directly back to an ADC and used as the reference signal to de-ramp the FMCW chirp. The other channel (surveillance) was connected to the RF front-end, up-mixed to 5.8 GHz (as previously described) and transmitted over the air. Return signal from the target was down-mixed by the front-end and sampled by a second ADC channel. Figure 7 shows the digital processing chain for the active radar implemented in the RFSoC hardware. Post-digitisation, the received data from both ADCs was digitally down-mixed and decimated by a factor of 8 on the RFSoC's RF tile. The remainder of the post-processing was then implemented in the FPGA fabric, where the two channels were digitally mixed together to extract the beat frequency (standard FMCW de-ramping or de-chirping methodology) before being further decimated by a factor of 64. This resulted in a complex signal sampled at 1.8 MHz, giving sufficient bandwidth to record the beat frequencies for the chirp period, bandwidth and target ranges used. The de-ramped signal was stored to DDR memory for offline post-processing as well as being passed into a hardware FMCW processing chain implemented in the FPGA. This applied a Hanning window to the data, performed an FFT and converted the result to a magnitude in dB, thus providing real-time RTI (range, time, intensity) data. This was live-streamed off of the RFSoC via Ethernet and used to provide real-time plots of the active radar data during the experiments. The real-time data is a useful capability, but was only used to guide the experiments and is not presented here.

Snapshots in time of a passive radar measurement of a

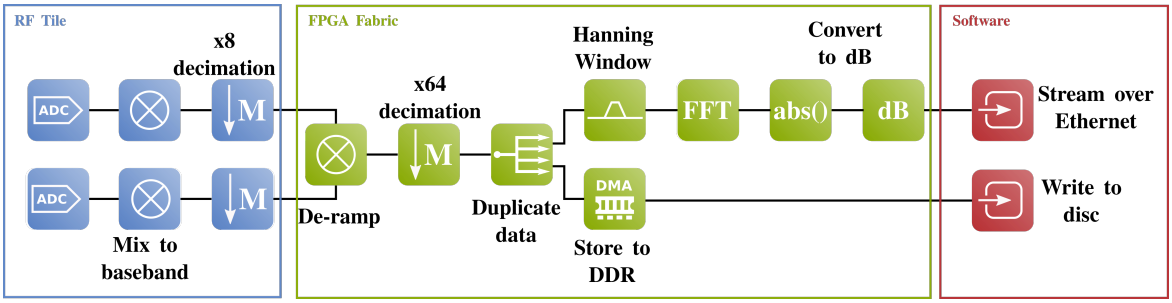

Fig. 7. Block diagram of the digital processing chain for the active FMCW radar showing the partitioning of processing steps between different elements of the RFSoC.

walking person can be seen in Fig. 8. The plots are of range vs. Doppler and are not normalised across time. The range bins are 2.5 m in size and the target therefore progresses from approximately 2.5 m bistatic range to 35 m over the 20 seconds duration from the first example range-Doppler slice to the last. The target in the centre of the image is a person walking away from the sensor in a triangle geometry between IoO, target & receiver antenna. The Doppler broadening is produced by the micro-Doppler of the target as they walk away from the sensor as their arms and legs move. During the same experiment the active FMCW mode was also running and the results are shown in Fig. 9. This is plotted as range vs. time after Moving Target Indicator (MTI) processing is applied. The 5 GHz ISM band allows for a wider bandwidth (150 MHz) and hence provides improved range resolution compared to the passive radar result. The active and passive radar measurements shown in Fig. 9 have been co-registered by subtracting the zero-range offsets (caused by the cables to the antennas) and converting the passive data to range rather than bistatic range. There is a strong agreement in the target position over the whole capture with small deviations of ∼1-2m. This could be further improved via filtering these raw detections via a joint tracker solution.

IV. Conclusions

Within this paper we have shown that it is possible to configure an RFSoC as a joint active passive RF sensor which can operate both modes simultaneously. Measurements of a walking person were performed using the ARESTOR system, with a WiFi router as the illuminator of opportunity along with a 5.8 GHz FMCW active radar waveform. Range profiles from the active and passive measurements were shown to be in good agreement with each other. The ability to operate in a dual active passive mode is expected to be a critical capability for future military platforms and de-risking of how best to operate in these different modes is best validated experimentally. Initial operational capabilities have demonstrated that the ARESTOR system is suitable to function as such an experimental testbed.

Future work may look towards learning when to be passive and when to be active within any given scenario. Initially this could be achieved in a lower TRL investigation by recording both data streams and only using one or another in offline processing to prove the concept. This would then be developed up to including the decision making within a real-time loop. This moves towards the Haykin [8] perception-action cycle requirement of a cognitive radar solution. In order to achieve this algorithm development work will be required to include analysis of real-time data that extends beyond an individual pulse repetition interval (PRI). This will enable decisions on which mode to use at any given time as a given scenario progresses.

Acknowledgment

The authors would like to thank the supporters of the research shown within this work. This includes Defence and Security Accelerator (DASA), the US Airforce Research Laboratories (AFRL), the Air Force Office of Scientific Research (AFOSR) and the cyber security PETRAS hub.

References

[1] N. Peters, C. Horne, M. Ritchie, ”ARESTOR: A Multi-role RF Sensor based on the Xilinx RFSoC”, EuRAD 2021, London.
[2] D. Dhulashia, N. Peters, C. Horne, P. Beasley and M. Ritchie, ”Multi-Frequency Radar Micro-Doppler Based Classification of Micro-Drone Payload Weight”, Frontiers in Signal Processing, 1, 2021.
[3] Xilinx, “ZCU111 Evaluation Kit.” [Online]. Available: https://www.xilinx.com/products/boards-and-kits/zcu111.html
[4] Q. Chen, K. Chetty, K. Woodbridge and B. Tan, ”Signs of life detection using wireless passive radar,” 2016 IEEE Radar Conference (RadarConf), 2016, pp. 1-5.
[5] T. P. Wibowo, F. Y. Zulkifli, ”Design of FMCW Ground Penetrating Radar For Concrete Inspection At ISM Band 2.4–2.5 GHz,” 2019 IEEE Asia-Pacific Microwave Conference (APMC), 2019, pp. 1232-1234.
[6] P. J. Beasley, M. A. Ritchie, ”bladeRAD: Development of an Active and Passive, Multistatic Enabled, Radar System,” 2021 18th European Radar Conference (EuRAD), 2022, pp. 98-101.
[7] R. Fagan, F. C. Robey, and L. Miller, “Phased array radar cost reduction through the use of commercial rf systems on a chip,” in 2018 IEEE Radar Conference (RadarConf18), 2018, pp. 0935–0939
[8] J. Palmer, S. Palumbo, T.T. van Cao and S. Howard, ”A new Illuminator of Opportunity Bistatic Radar”, Research Project at DSTO, Electronic Warfare and Radar Division, Defence Science and Technology Organisation, DSTO–TR–2269
[9] S. Haykin, ”Cognitive Dynamic Systems: Perception-Action Cycle Radar and Radio” in , Cambridge University Press, 2011
[10] J. S. Sandenbergh and M. R. Inggs, ”A Summary of the Results Achieved by the GPS Disciplined References of the NetRAD and NeXtRAD Multistatic Radars,” 2019 IEEE Radar Conference (RadarConf), 2019, pp. 1-6.
[11] Z. Mathews, L. Quiriconi, C. Schüpbach, P. Weber, ”Learning Resource Allocation in Active-Passive Radar Sensor Networks”, Frontiers in Signal Processing, Vol 2, 2022

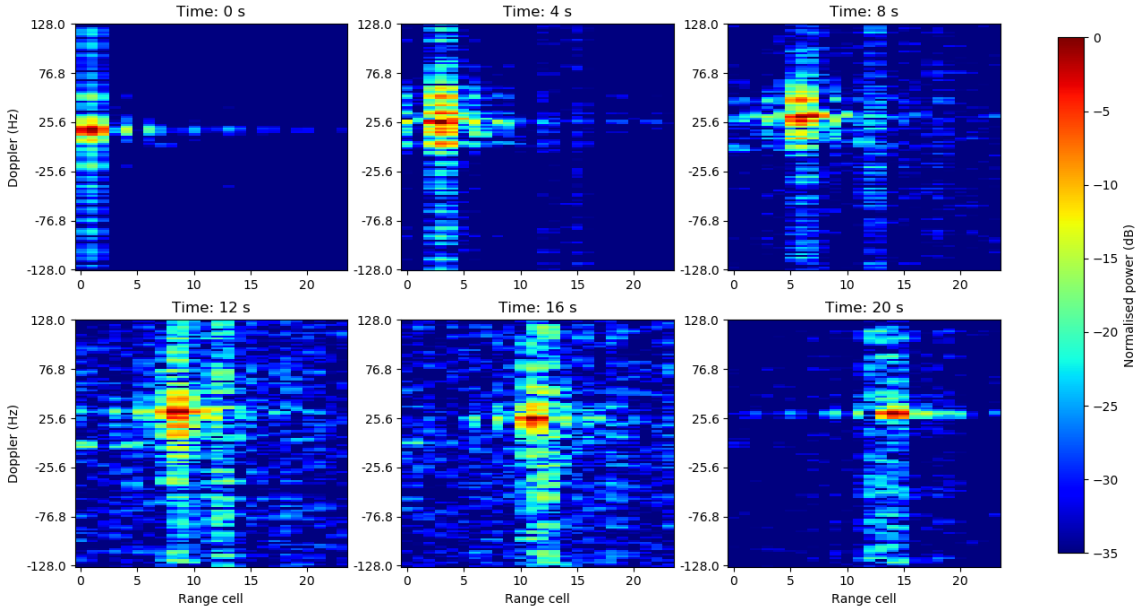

Fig. 8. Passive measurement of person walking. Results show a Range-Doppler surface. This used a WiFi illuminator at the 2.4 GHz ISM band.

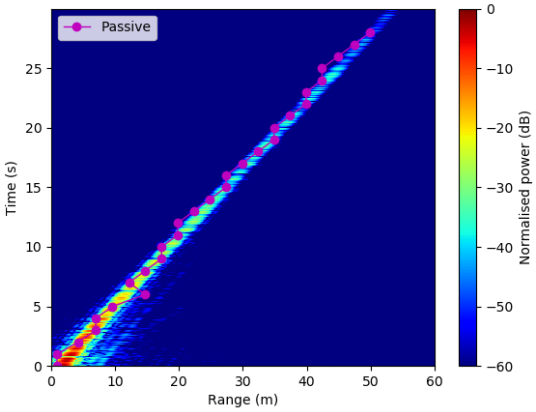

Fig. 9. Comparison of simultaneous active and passive radar detections of a walking person target. The active radar data has had MTI processing applied. Passive radar detections are found by applying a CFAR to the passive radar data (a subset of which is shown in Fig. 8).

[12] D. Dhulashia, M. Temiz and M. A. Ritchie, "Jamming Effects on Hybrid Multistatic Radar Network Range and Velocity Estimation Errors," in IEEE Access, vol. 10, pp. 27736-27749, 2022, doi: 10.1109/ACCESS.2022.3157607.

[13] U.S. Naval Research Laboratory, "Multi-Generator (MGEN) Network Test Tool", https://www.nrl.navy.mil/Our-Work/Areas-of-Research/Information-Technology/NCS/MGEN/

[14] P. Tamás, "pyAPRiL -Advanced Passive Radar Library", https://github.com/petotamas/APRiL

[15] G. Smith, K. Chetty, C. Baker and K. Woodbridge "Extended time processing for passive bistatic radar", IET Radar, Sonar and Navigation, vol. 7 issue 9, pp 1012-1018, 2013